



This is a repository copy of *CoFeMn<sub>0.5</sub>Al<sub>0.25</sub>: a high magnetisation CoFe based soft alloy with reduced Co content.*

White Rose Research Online URL for this paper:

<https://eprints.whiterose.ac.uk/197384/>

Version: Published Version

---

**Article:**

Rowan-Robinson, R.M., Leong, Z. and Morley, N.A. orcid.org/0000-0002-7284-7978 (2023) CoFeMn<sub>0.5</sub>Al<sub>0.25</sub>: a high magnetisation CoFe based soft alloy with reduced Co content. *Materials Chemistry and Physics*, 299. 127518. ISSN 0254-0584

<https://doi.org/10.1016/j.matchemphys.2023.127518>

---

**Reuse**

This article is distributed under the terms of the Creative Commons Attribution (CC BY) licence. This licence allows you to distribute, remix, tweak, and build upon the work, even commercially, as long as you credit the authors for the original work. More information and the full terms of the licence here:

<https://creativecommons.org/licenses/>

**Takedown**

If you consider content in White Rose Research Online to be in breach of UK law, please notify us by emailing [eprints@whiterose.ac.uk](mailto:eprints@whiterose.ac.uk) including the URL of the record and the reason for the withdrawal request.



[eprints@whiterose.ac.uk](mailto:eprints@whiterose.ac.uk)  
<https://eprints.whiterose.ac.uk/>



# CoFeMn<sub>0.5</sub>Al<sub>0.25</sub>: A high magnetisation CoFe based soft alloy with reduced Co content

R.M. Rowan-Robinson, Z. Leong, N.A. Morley\*

Department of Material Science and Engineering, University of Sheffield, Sheffield, S1 3JD, UK

## HIGHLIGHTS

- CoFeMn<sub>0.5</sub>Al<sub>0.25</sub> has competitive soft magnetic properties with CoFe but lower cost.
- Alloys with Al < 0.2 had FCC and BCC phases and low magnetisation.
- Alloys with Al > 0.25, contained only BCC and had the largest magnetisation.
- Alloys with Al < 0.75 had Curie temperatures higher than 1000 K.

## ARTICLE INFO

### Keywords:

High entropy alloys  
Soft magnetic materials  
Multi-component alloys

## ABSTRACT

The high cost of CoFe alloys has prevented their widespread use regardless of their promising properties such as high magnetisation, high Curie temperature, as soft magnetic materials for high temperature applications. Here, it is shown that AlMn can be used to create a CoFeMn<sub>0.5</sub>Al<sub>x</sub> alloy, which has reduced Co content but comparable soft magnetic properties as CoFe alloys, therefore providing a more economical alternative to pure CoFe soft magnets.

## 1. Introduction

CoFe is one of the most commonly used soft magnetic materials, due to its high saturation magnetisation (1910 kA/m (228 Am<sup>2</sup>/kg)) and low coercive field (150 A/m) [1,2]. This means it is found in applications such as high performance transformers, internal starters for aircraft and magnetostrictive transducers [2]. One of its limiting factors for wider use is the cost of the Co, which at the present is 52 \$/kg, but has fluctuated between 23 \$/kg and 110 \$/kg over the past 10 years [3,4]. This uncertainty in the price along with being over 200 times more expensive than Fe ore (0.11 \$/kg) [3], means that cheaper inferior alloys are often utilised, at the expense of operation efficiency. Further CoFe tends to fracture with a low yield strength and ductility [5]. Thus previous works on CoFe have studied adding 2% of more economical elements such as V or Nb in, to improve the mechanical properties [5,6], while aiming to maintain the soft magnetic properties [6]. The addition of 2% V has a small effect on the saturation magnetisation, reducing it by less than 5%, but often increases the coercive field by an order of magnitude, making the alloy unfavourable for most soft magnetic applications. The mechanical properties can be improved, but the issue around cost still

remains, as most CoFe alloys still contain over 45% Co. While other researchers have studied amorphous CoFe to achieve softer magnetic properties, with the addition of Nd, B, Zr etc [7]. The amount of Co in these is reduced to between 20 and 40%, but B is expensive (100 \$/kg), and the processing procedures are more costly, so these amorphous alloys are often only used in specific applications.

New alloys are being designed to reduce the amount of Co in soft magnetic alloys by substituting it with cheaper elements, while maintaining the magnetic properties. This means there are a limited number of elements that can be added, with Mn (2.20 \$/kg) and Al (2.33 \$/kg) being the most popular. The majority of the research on CoFeMnAl has been done under multi-component alloys (MCAs) research including high entropy alloys (HEA), where the alloys contain 4 or more elements in equimolar or close to equimolar amounts. These alloys often have single solid solutions, due to the high entropy of mixing of the elements, the sluggish diffusion kinetics and cocktail effect [8,9]. They are dynamic alloys, for which the magnetic properties can be dramatically altered through the composition, often as a result of competing structural phases, as showcased in the tuneable Curie temperature and saturation magnetisation in the CoFeNiAlCr system [10,11]. There has

\* Corresponding author.

E-mail address: [n.a.morley@sheffield.ac.uk](mailto:n.a.morley@sheffield.ac.uk) (N.A. Morley).

<https://doi.org/10.1016/j.matchemphys.2023.127518>

Received 29 October 2022; Received in revised form 16 January 2023; Accepted 15 February 2023

Available online 19 February 2023

0254-0584/© 2023 The Authors. Published by Elsevier B.V. This is an open access article under the CC BY license (<http://creativecommons.org/licenses/by/4.0/>).

been a large focus on the mechanical properties of HEAs [9,12], with research showing that the phase or phases present in the alloy strongly influences the mechanical properties. For example, FCC alloys have high ductility, but low yield strength, while BCC alloys have the opposite with high yield strength, but poor ductility, such that when alloys are designed to contain both phases, then the combination gives alloys with high yield strength and good ductility [9]. Therefore it is likely that any new magnetic HEA discovered is likely to have better mechanical properties than CoFe.

The majority of the research studied in magnetic HEAs uses CoFeNi as the base elements, with the addition of other non-magnetic elements, such as Mn, Al, Si, Ga, Cr etc [13]. Li et al., [14] studied the alloy series  $\text{CoFeNi}(\text{MnAl})_x$  and determined that as  $x$  increased, the phases went from FCC to FCC + BCC mixed to BCC, with the magnetisation decreasing until  $x = 0.5$  (mixed FCC + BCC) and then increasing again as the alloy became BCC. The saturation magnetisations were relatively high, with values of  $156 \text{ Am}^2/\text{kg}$  for  $x = 0$  and  $132 \text{ Am}^2/\text{kg}$  for  $x = 1$ , plus the coercive field for these alloys were small ( $189 \text{ A/m}$  for  $x = 0$  and  $266 \text{ A/m}$  for  $x = 1$ ). While Harharan et al., [15] studied  $\text{CoFeNiMnAl}_x$  alloy series, and found that additions of Al induced magnetisation into the alloys at room temperature, with the  $\text{CoFeNiMnAl}$  alloy having the largest magnetisation at room temperature of  $126 \text{ Am}^2/\text{kg}$ . Zuo et al., [16] determined the magnetic properties of  $\text{CoFeNiMnAl}$  to be a magnetisation of  $148 \text{ Am}^2/\text{kg}$  and a coercive field of  $629 \text{ A/m}$ . Thus the addition of MnAl shows promising magnetic results.

## 2. Design

Al-containing MCAs stabilise the BCC structure which coherently exists with an ordered B2 structure ( $\text{AlCo/AlNi}$  etc.) [17] and initial formation of the BCC/B2 structure increases magnetisation while further Al paramagnetic addition reduces it [18]. Morley et al. [10] reported that compositional tuning of a  $\text{CoCrFeNi-Al}$  to increase magnetisation through nanoprecipitation and BCC/B2 phase separation. In their work, the separation was found to be driven by Al-Co and Al-Ni ordering, with FeCr based particles forming. In order to further increase magnetisation, the deleterious effect of Cr should be reduced as addition of Cr is detrimental to the saturation magnetisation magnitude, with even small amounts of Cr strongly affecting magnetic properties [10, 19]. Ni is one of the magnetic transition metals, but at the present time (2022: 22 \$/kg), the costs associated with it are increasing, also Ni has an atomic moment of  $0.61 \mu\text{B}$ , which is less than half Co ( $1.72 \mu\text{B}$ ) and Fe ( $2.22 \mu\text{B}$ ), and therefore again adding it to the HEAs tends to decrease the saturation magnetisation.

We hypothesised that 1) Antiferromagnetic Cr may be replaced with Mn to reduce the antiferromagnetic component of the final alloy; 2) This composition can be tuned to maintain the strategy of driving Al-X B2 separation from the parent matrix in order to introduce lattice strain into the matrix, which increases magnetisation.

These elemental choices (Co, Fe, Mn, and Al) make sense since Mn and Al are economically viable with costs of  $2.20 \text{ $/kg}$  and  $2.33 \text{ $/kg}$  respectively. Although Mn is not ferromagnetic in elemental form, it is known to take on a large moment when alloyed. For example, MnAl has been the subject of research for rare-earth free permanent magnets and the total moment of  $\text{Co}_2\text{MnAl}$  heusler alloys has a strong contribution from ferromagnetic polarisation at the Mn sites. This spontaneous ferromagnet polarisation been shown in HEAs by Zuo et al., [16] where the magnetic moment for each atom was determined for  $\text{CoFeNiMnAl}$ , with the Mn having the largest moment *per* atom and the Ni's moment *per* atom was almost zero.

To narrow down potential compositional choices, we ran a number of semi-empirical calculations following the methodology used in Ref. [19] to determine the probability of binary pair formation for  $\text{CoFeMn}_x\text{Al}_y$  compositions where we determined that 1) Unlike Cr, Mn competes with Co in forming binary pairs with Al (both have enthalpy of mixing values of  $-19 \text{ kJ/mol}$ ); 2) The total magnetic contribution of the

binary pairs are higher than when all the elements are in solid solution; 3) The average magnetisation increases by 25% when comparing  $\text{CoFeMn}_{0.5}\text{Al}$  to  $\text{CoFeMnAl}$ ; 4) The magnetisation increase for precipitation from solid solution is maximised for  $\text{CoFeMn}_{0.5}\text{Al}_x$  for  $0.25 < x < 0.75$ . In this new composition we would thus expect the formation of Al-Co and Al-Mn segregation on Al addition, and the addition of Mn increases the availability of Co to retain FeCo pairs, which will have a higher magnetisation than the FeCr phase found in Ref. [10].

Guided by the above design choices, the experimental work in this study therefore focuses on the base alloy  $\text{CoFeMn}_{0.5}$  with the addition of Al, to determine how the cheaper non-magnetic elements can be used to change the magnetic properties, while reducing the percentage of Co, thus decreasing the cost of the alloy.

## 3. Materials and methods

To fabricate the alloys, pellets and foils of the four elements with 99.99% purity were weighed out for the required compositions (see Table 1). The elements were then arc-melted at least three times in an Edmund Buhler compact arc-melter, to ensure homogeneity. The final sample of each composition was a button ingot. No further heat treatments were carried out, as the work focused on the as-synthesised alloys.

A range of techniques were used to characterise the alloys. This included x-ray diffraction using Bruker D1 and Panalytical X'pert diffractometers, in both cases using  $\text{Cu K}\alpha$  radiation. Scanning electron microscopy (SEM) to study the grains and microstructure, with energy dispersive x-ray (EDX) to determine the composition. The magnetic properties were measured using a MPMS-3 SQUID magnetometer, as a function of magnetic field up to 3 T and temperature up to 950 K. From the magnetisation hysteresis loops the saturation magnetisation ( $M_s$ ), coercive field ( $H_c$ ) and remanent magnetisation ( $M_r$ ) were determined at room temperature. The magnetisation as a function of temperature data, were taken at  $40 \text{ kA/m}$  and  $2390 \text{ kA/m}$  up to 950 K. The Curie temperature is normally determined from this magnetisation vs temperature data, but for these alloys the Curie temperature was above 950 K, thus Bloch law was used to estimate it [20].

## 4. Results

After synthesis, the composition of each of the alloys was determined from the EDX data (Table 1). It is observed that for all the alloys, the Al concentrations are lower than the nominal concentrations, but do increase with the expected differences. Also at the lower Al concentrations the Mn percentage is lower than the nominal, but is about right for the higher Al concentrations. This is likely to have arisen during the arc-melting with the Mn evaporating away during the process. Further the Co and Fe concentrations are always higher than the nominal values, with Fe always higher than the Co. Table 1 also gives the sample abbreviations used in the rest of the paper.

From the SEM backscattered images (Fig. 1), it is observed for the Al0 alloy, that Co is evenly distributed, while there are regions that are Mn rich and regions that are Fe rich, which is also observed for the Al0.16 alloy as well. For  $x > 0.25$ , all the elements are more homogeneously distributed in the alloys. Elemental distribution appears to be present for the Al composition, and image analysis techniques were used [10] to determine the elemental pairing within the system by comparing the relative intensities for each EDS image in 2D coordinate space between each element. The analysis showed 1) No strong Al-Co pairing, which agrees with the pair analysis done during the design process – this is because Co is in excess and is not used up by the Al addition and it may thus be inferred that Co distributed throughout the sample; 2) Fe-Mn and Co-Mn pairing reduces from Al0.13 onwards, which again agrees with the design hypothesis as Fe-Mn and Co-Mn enthalpy of mixing values are far lower than Al-Mn (cf Fig. 2c) while the inverse is true for Al-Mn. These results are in good agreement with the hypothesis of this work.

**Table 1**  
Composition of the  $\text{CoFeMn}_{0.5}\text{Al}_x$  samples.

Alloy (Abbreviation)	Nominal Composition				Actual Weight Percentage (%)				Normalised Molar percentage
	Co	Fe	Mn	Al	Co	Fe	Mn	Al	
$\text{CoFeMn}_{0.5}$ (A10)	40	40	20	0	43.3	41.3	15.4	0	$\text{Co}_{0.99}\text{FeMn}_{0.38}$
$\text{CoFeMn}_{0.5}\text{Al}_{0.15}$ (A10.13)	37.7	37.7	18.9	5.7	40.7	41.6	15	2.7	$\text{Co}_{0.93}\text{FeMn}_{0.37}\text{Al}_{0.13}$
$\text{CoFeMn}_{0.5}\text{Al}_{0.2}$ (A10.16)	37	37	18.5	7.5	39.9	41.1	15.8	3.2	$\text{Co}_{0.92}\text{FeMn}_{0.39}\text{Al}_{0.16}$
$\text{CoFeMn}_{0.5}\text{Al}_{0.25}$ (A10.25)	36.4	36.4	18.2	9	40.2	38.7	16.4	4.7	$\text{Co}_{0.98}\text{FeMn}_{0.43}\text{Al}_{0.25}$
$\text{CoFeMn}_{0.5}\text{Al}_{0.5}$ (A10.47)	30.8	30.8	15.4	23	38	37.2	16.4	8.4	$\text{Co}_{0.97}\text{FeMn}_{0.45}\text{Al}_{0.47}$
$\text{CoFeMn}_{0.5}\text{Al}_{0.75}$ (A10.71)	33.3	33.3	16.7	16.7	36.6	35.2	16.2	12	$\text{Co}_{0.99}\text{FeMn}_{0.47}\text{Al}_{0.71}$

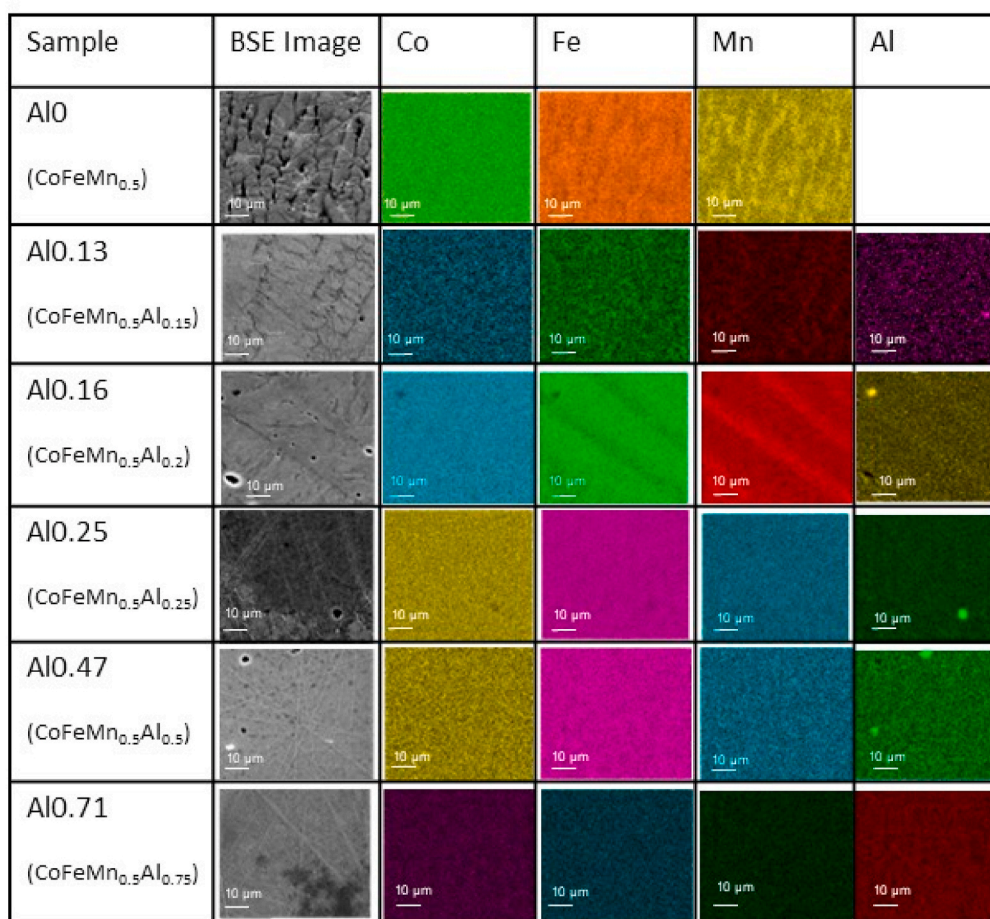


**Fig. 1.** SEM backscattered and EDX images of A10 ( $\text{CoFeMn}_{0.5}$ ), A10.13 ( $\text{CoFeMn}_{0.5}\text{Al}_{0.15}$ ), A10.16 ( $\text{CoFeMn}_{0.5}\text{Al}_{0.2}$ ), A10.25 ( $\text{CoFeMn}_{0.5}\text{Al}_{0.25}$ ), A10.47 ( $\text{CoFeMn}_{0.5}\text{Al}_{0.5}$ ) and A10.71 ( $\text{CoFeMn}_{0.5}\text{Al}_{0.75}$ ).

The phases present in the alloy were determined from the XRD (Fig. 2a). It is observed that for  $x < 0.2$ , there exists a dominant BCC phase and a smaller FCC phase. Previous work on  $\text{CoFeNiMnAl}$  alloys, have also observed these mixed phases [15]. For  $x > 0.2$  only a BCC phase is observed, thus the addition of Al stabilises the BCC phase within the alloy. For the A10.71 sample, two BCC phases are measured, which could be a BCC/B2 mix, due to phase segregation driven by the Al, as predicted in the research design. From the XRD data, the lattice constants (Fig. 2b) and the crystalline sizes using Scherer equation (Table 2) were determined. The BCC lattice constants in general increased with Al addition. For all the alloys, the crystallite size was  $\sim 30$  nm, suggesting that the Al has stabilised the BCC phase, but hasn't driven the formation of nanoparticles, which has been observed in other HEA alloy systems [10,19]. The VEC (valence electron concentration) was determined for each of the alloys (Table 2). This is a parameter used within HEAs to determine the likely phases present in the alloy [21]. In general, a VEC

$> 8$  leads to FCC phases, while a VEC  $< 6.87$  gives BCC phases. The VECs determined for the  $\text{CoFeMn}_{0.5}\text{Al}_x$  range from 8.2 for the A10 alloy, which had a mixed FCC and BCC phase to 7 for the A10.71 alloy, which had two BCC phases. These are slightly different from the predictions, but this does explain why a FCC phase is observed within the lower Al concentration alloys.

Using pair analysis [19], which uses the binary enthalpy of mixing for atomic pairs as extracted from Miedema's model [22,23] (Fig. 2c) to predict the probability of element pair formation, i.e. the likelihood of the element pairs Al–Mn and Al–Co forming in the alloy. It was found that with no Al in the alloy then the Co–Mn is likely to form pairs, as these have the more negative enthalpy of mixing. This is observed in the back-scattered electron images (Fig. 1), where for the A10 sample, Co is homogeneously distributed, while regions of Fe and Mn exist, such that they are the “negatives” of each other. With the addition of Al, the Al is likely to pair with the Co and the Mn, as both these pairings similarly

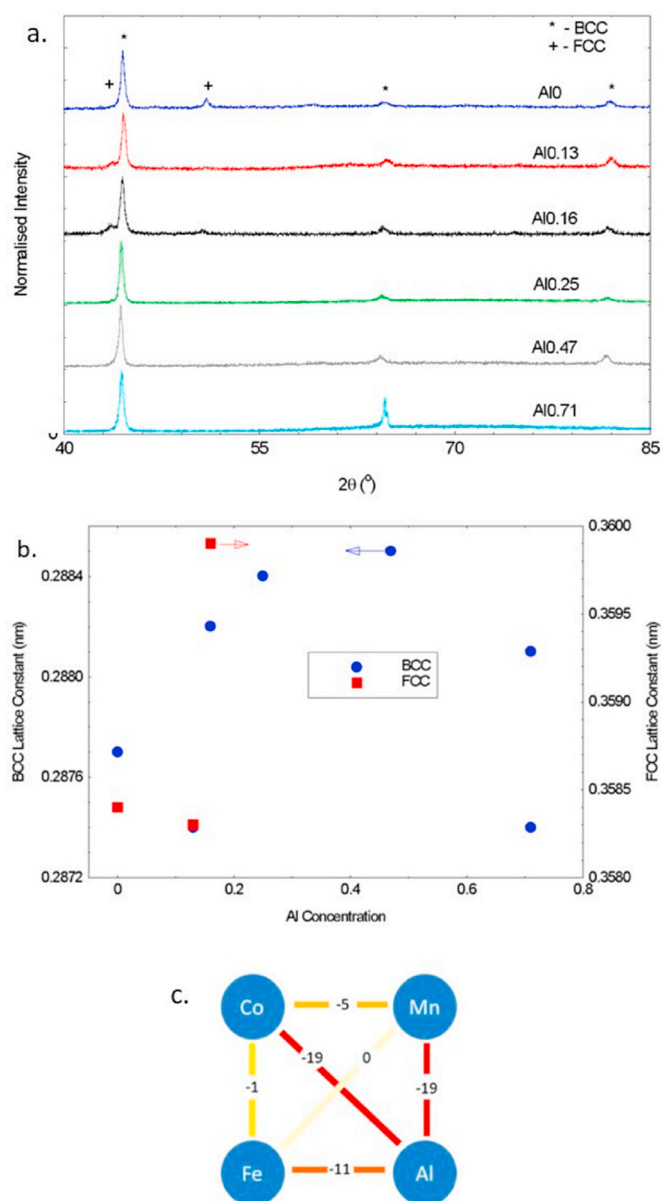


**Fig. 2.** a. XRD patterns for the CoFeMn<sub>0.5</sub>Al<sub>x</sub> samples, where the patterns are normalised to the highest peak, and then each pattern is offset along the y-axis. 2b. Lattice constant as a function of Al concentration, and 2c Enthalpy of mixing diagram for CoFeMnAl.

**Table 2**  
Structural Parameters of the CoFeMn<sub>0.5</sub>Al<sub>x</sub> samples.

Alloy (sample)	VEC (e/a)	Lattice Constant (nm)	Phase	Crystallite size (nm)
Al0 (CoFeMn <sub>0.5</sub> )	8.2	0.2877 0.3584	BCC FCC	28 ± 1 21 ± 5
Al0.13 (CoFeMn <sub>0.5</sub> Al <sub>0.15</sub> )	8	0.2874 0.3583	BCC FCC	28 ± 1 31 ± 3
Al0.16 (CoFeMn <sub>0.5</sub> Al <sub>0.2</sub> )	7.9	0.2882 0.3599	BCC FCC	25 ± 1 13 ± 2
Al0.25 (CoFeMn <sub>0.5</sub> Al <sub>0.25</sub> )	7.7	0.2884	BCC	34 ± 1
Al0.47 (CoFeMn <sub>0.5</sub> Al <sub>0.5</sub> )	7.4	0.2885	BCC	31 ± 1
Al0.71 (CoFeMn <sub>0.5</sub> Al <sub>0.75</sub> )	7	0.2881 0.2874	BCC BCC	29 ± 1

negative values of enthalpy of mixing, while reducing the likelihood of Fe-Mn/Fe-Co pairs. It is worth mentioning again that the alloying strategy here involves 1) Maintaining a source of Co for Co-Fe pairing to occur with the addition of Mn, 2) Introducing Al to form Al-Co and Al-Mn pairs that stabilise the B2 phase which co-exists with the BCC phase. The increased incoherency of the B2/BCC interface introduces lattice strain which can modify magnetisation.

Relating the EDS analysis performed earlier to the phases observed in the alloys, Fe and CoMn tend to both be BCC, while CoFe, where the concentration of Fe is less than 20% gives an FCC phase. As expected, the addition of Al may therefore act to remove the Co from the CoFe phase to form a BCC CoAl phase, and thus leaving a BCC CoFe phase, which could be the two BCC phases observed in the highest Al containing alloys (Al0.71).

The magnetic hysteresis loops were measured as a function of applied magnetic field at 300 K. From Fig. 3a, it is observed that the saturation magnetisation depends on both the alloy composition and the phases present in the alloy. For the alloys with  $x < 0.2$ , the saturation magnetisation decreased as the Al concentration increased, with all these alloys containing a BCC and FCC phase (Fig. 2a). For the Al0.25 alloy, the saturation magnetisation increased, compared to the parent alloy Al0, although there are more non-magnetic elements within the alloy. This could be due to the alloy only containing BCC phases suggesting the removal of the FCC phase from within the alloy coincides with an increase in the saturation magnetisation. This effect was also observed by Li et al. [14] in the CoFeNi(MnAl)<sub>x</sub> series. However, it could arise from ferromagnetic polarisation of the Mn atoms, as proposed by Zhu et al. who used ab-initio calculations to support their conclusion for the CoFeNiMnAl system [16]. Validation of these hypotheses would require element specific scattering techniques available only at central x-ray/neutron facilities. Crucially, it is clear that MnAl formation can be used in this way to reduce the Co content in these alloys without sacrificing saturation magnetisation. Furthermore, the coercive field is smaller for the Al0.25 sample, providing additional benefit for soft magnetic material applications. In addition, removing the Ni from the base magnetic alloy has increased the saturation magnetisation at room temperature, without changing the coercive field, with both the Al0.25 and Al0.47 ( $x = 0.25$  and  $0.5$ ) samples having higher magnetisations than those of CoFeNiMnAl (~130 Am<sup>2</sup>/kg) [14,15].

A second set of magnetisation hysteresis loops were measured (Fig. 3b), after the magnetisation vs. temperature measurements were carried out (Fig. 3c and d). As no heat treatment was carried out after the samples were synthesised, it is possible that the as-synthesised samples were not in an equilibrium microstructural state. Thus the temperature measurement to determine the Curie temperature could change the phases and/or proportion of the phases present in the samples. Due to the small size of the heated SQUID samples, it was not possible to collect structure data using the XRD, but the magnetic properties could be remeasured. It is observed in Fig. 3b, for the  $x < 0.2$  samples that the saturation magnetisation decreases and the coercive field increases after heating. These samples have both a BCC and FCC phase, so this is probably due to the growth of the “lower-/non-magnetic” phase in relation to the higher magnetic phase. For the  $x > 0.5$  samples, the heating procedure did not affect the saturation magnetisation nor the coercive field, as both were the same after heating, meaning they were already in an equilibrium state. For the Al0.25 alloy, the saturation magnetisation and coercive field both decreased. This suggests that the BCC phase could be unstable, which is possible as the VEC = 7.7, which is much higher than the VEC = 6.87 expected for the BCC phase, and closer to the VEC > 8 for the FCC phase. Further heat treatment work would have to be carried out to confirm this.

Another important parameter for CoFe based alloys is the Curie temperature, as they are often used in high temperature applications. The Curie temperature was determined from the magnetisation vs temperature data (Fig. 3c and d). The measurement was taken up to 950 K, as this was the highest temperature available on the SQUID system. As

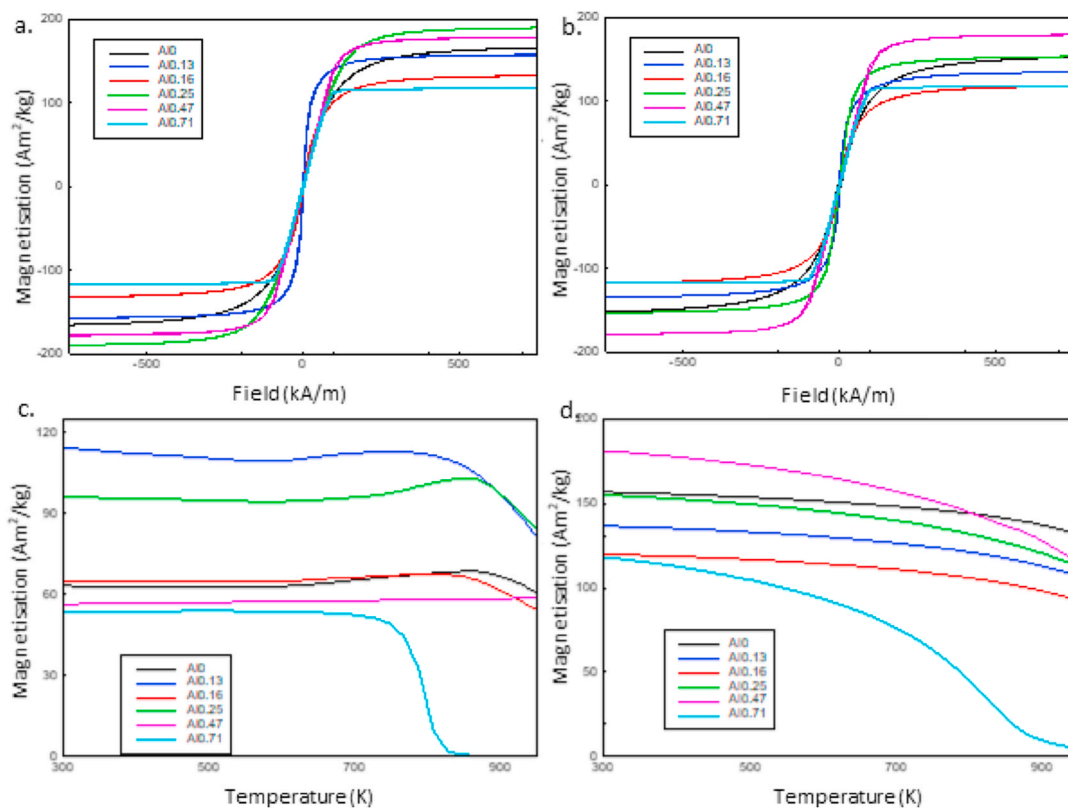


**Fig. 3.** a. Magnetisation as a function of magnetic field for the  $\text{CoFeMn}_{0.5}\text{Al}_x$  samples before heating to 950 K. b. Magnetisation as a function of magnetic field for the  $\text{CoFeMn}_{0.5}\text{Al}_x$  samples after heating to 950 K. c. Magnetisation as a function of temperature for an applied field of 40 kA/m for the  $\text{CoFeMn}_{0.5}\text{Al}_x$  samples. d. Magnetisation as a function of temperature for an applied field of 2390 kA/m for the  $\text{CoFeMn}_{0.5}\text{Al}_x$  samples.

only the Al0.71 sample showed a transition from ferromagnetic to paramagnetic within this temperature range, Bloch law was used to estimate the Curie temperature for the other samples. CoFe has a Curie temperature of 1253 K, so anything over 1000 K, allows the materials to be used in high temperature applications. From Table 3, it is observed that the Curie temperature of 4 out of the 5 new alloys studied were higher than 1000 K, so maintaining the high transition temperature, and allowing them to be used in high temperature applications. There is a reduction in the Curie temperature compared to CoFe for all of the samples, but this is likely due to the addition of the non-magnetic elements. Also as expected the alloy with the highest concentration of Al, has the lowest Curie temperature.

The saturation magnetisation of the system can be correlated to the

**Table 3**  
Magnetic Parameters of the  $\text{CoFeMn}_{0.5}\text{Al}_x$  samples.

Alloy (sample)	Saturation Magnetisation ( $\text{Am}^2/\text{kg}$ )		Coercive Field (A/m)		Curie Temperature <sup>a</sup> (K)
	Before	After	Before	After	
Al0 (CoFeMn <sub>0.5</sub> )	170	156	636	4377	1044
Al0.13 (CoFeMn <sub>0.5</sub> Al <sub>0.15</sub> )	159	138	796	1472	1074
Al0.16 (CoFeMn <sub>0.5</sub> Al <sub>0.2</sub> )	134	119	716	1830	1055
Al0.25 (CoFeMn <sub>0.5</sub> Al <sub>0.25</sub> )	191	155	159	40	1097
Al0.47 (CoFeMn <sub>0.5</sub> Al <sub>0.5</sub> )	181	181	2387	2387	1055
Al0.71 (CoFeMn <sub>0.5</sub> Al <sub>0.75</sub> )	117	117	2706	2706	787 (826 <sup>b</sup> )

<sup>a</sup> Estimated from Bloch law.

<sup>b</sup> Determined from data.

Wigner-Seitz radii (i.e. the average volume occupied *per* atom in the lattice structure) of the alloy, which can be calculated from the experimentally determined lattice parameters. Fig. 4a shows that the experimental magnetisation is located near the parabolic maximum of the achievable Wigner-Seitz radius with respect to Al addition. The parabolic maximum of a Wigner-Seitz radius for a particular lattice parameter is normally linked to lattice stress accommodated in a system prior to strain release through some mechanism such as precipitation; it has been reported that this excess energy can act as a driving force to increase magnetisation in the system [10]. From the calculations, the CoFe remaining in the solid solution (ie. Non Al-containing binaries) can be determined and its magnetisation estimated using the well-known Slater-Pauling relationship. This is plotted in Fig. 4b which shows that the predicted magnetisations are modified from the experimentally determined magnetisations for the compositions which lie near the Wigner-Seitz maxima location. Furthermore, from the experimental results, the compositions with the FCC structure are Al0, Al0.13, and Al0.16 and therefore the Al0.13–0.25 region may be regarded as the compositions where the FCC structure transitions to the BCC structure, hence act as the region of increased stress. This agrees well with the predictive model that was used to design this alloy system.

Fig. 5 compares the soft magnetic properties of the new CoFeMnAl alloys with the existing soft magnetic alloys. Saturation induction is plotted rather than magnetisation, as this is the value that is often quoted for commercial products. It is observed that CoFe has the largest induction (2.4 T) and one of the smallest coercive field (150 A/m). The addition of 2% of a non-magnetic alloy decreases the induction by 3%, but increases the coercive field up to 22 times larger. While amorphous alloys, such as FeCoZrBCu [7] and FeCoNbB [24] have the smallest coercive fields (7 times smaller), but also a reduction in the induction of 31%. For the HEAs (CoFe(Ni)MnAl), the inclusion of Ni reduces the induction, but helps to maintain a small (<1000 A/m) coercive field.

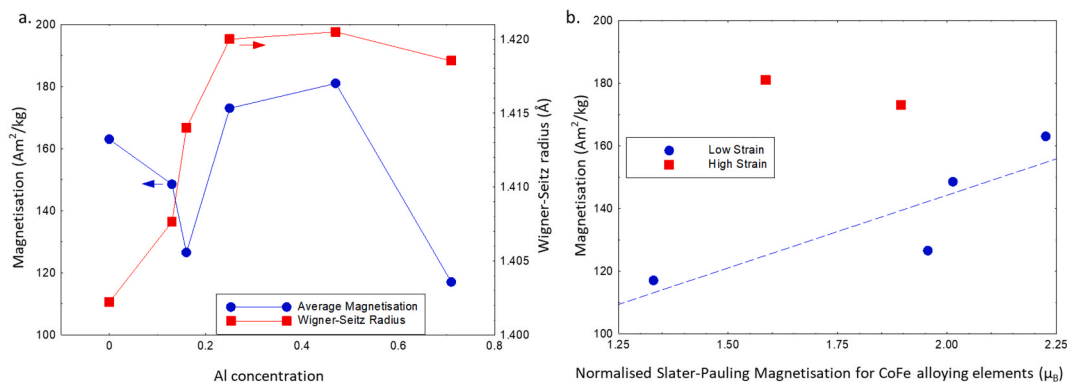


**Fig. 4.** a. Magnetisation and Wigner-Seitz radius as a function of Al concentration. 4b. Magnetisation as a function of the Normalised Slater-Pauling Magnetisation for the CoFe alloying elements. The dashed line is a linear fit to the low strain data.

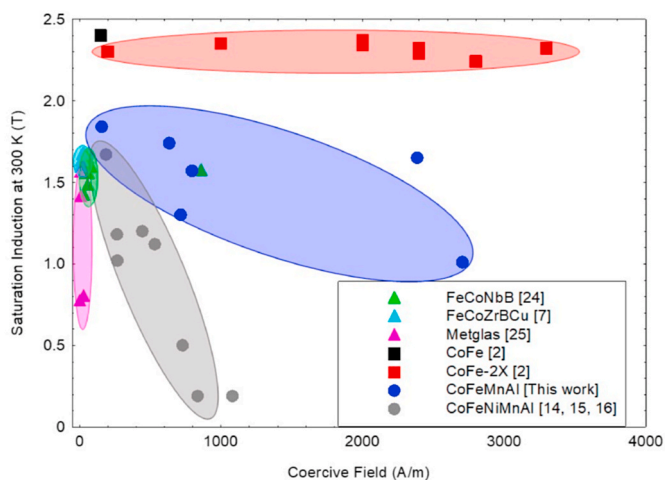


**Fig. 5.** Saturation induction as a function of coercive field for the CoFeMn<sub>0.5</sub>Al<sub>x</sub> alloys and other soft magnetic alloys. The square shapes are the FeCo based alloys, the circle shapes are the HEAs and the triangular shapes are amorphous alloys. Each ellipsis encloses the majority of the data points for each data set, and are there as a guide for the eye. The data for the alloys are taken from the following publications: FeCoZrBCu - [7]; FeCoNbB - [24]; Metglas - [25]; CoFe, CoFe-2X - [2]; CoFeMnAl - this work; CoFeNiMnAl - [14–16].

While the removal of Ni increases the induction, but also increases the coercive field. The HEAs with the highest induction, also had the smallest coercive field. The induction was 23%–31% lower than CoFe, but higher than the amorphous alloys plus the coercive field was the same as CoFe. Thus the magnetic properties of the CoFeMn<sub>0.5</sub>Al<sub>x</sub> alloys are competitive with existing CoFe based alloys. Using the prices quoted in the introduction the cost of CoFe raw materials is 26 \$/kg, with the new alloy that drops by ~30% to 18 \$/kg.

## 5. Conclusions

The addition of inexpensive MnAl to CoFe not only maintains the soft magnetic properties of the magnetic alloy, but also reduces its cost. The addition of Al to the base alloy CoFeMn<sub>0.5</sub>, helped to stabilise the BCC phase within the alloy, which increased the saturation magnetisation, while decreasing the coercive field. This led to two alloys, Al<sub>0.25</sub> and Al<sub>0.47</sub>, having competitive magnetic properties at 300 K, along with Curie temperatures higher than 1000 K, making them a possible candidate for high temperature applications, such as power transformers and inductors.

## CRedit authorship contribution statement

**R.M. Rowan-Robinson:** Conceptualization, Data curation, Formal analysis, Investigation, Methodology, Resources, Validation, Roles, Writing – original draft, Writing – review & editing. **Z. Leong:** Conceptualization, Formal analysis, Writing – review & editing. **N.A. Morley:** Conceptualization, Formal analysis, Funding acquisition, Project administration, Resources, Supervision, Roles, Writing – original draft, Writing – review & editing.

## Declaration of competing interest

The authors declare that they have no known competing financial interests or personal relationships that could have appeared to influence the work reported in this paper.

## Data availability

Data will be made available on request.

## Acknowledgments

This work was supported by the Royal Society Mid-Career Leverhulme Trust Fellowship scheme (SRF\R1\180020) and the Leverhulme Trust (RPG-2018-324).

## References

- [1] D.I. Bardos, Mean magnetic moments in bcc Fe–Co alloys, *J. Appl. Phys.* 40 (1969) 1371, <https://doi.org/10.1063/1.1657673>.
- [2] R.S. Sundar, S.C. Deevi, Soft magnetic FeCo alloys: alloy development, processing and properties, *Int. Mater. Rev.* 50 (3) (2005) 157–192, <https://doi.org/10.1179/174328005X14339>.
- [3] <https://www.dailymetalprice.com/>.
- [4] <https://uk.investing.com/commodities/>.
- [5] E.P. George, A.N. Gubbi, I. Baker, L. Robertson, Mechanical properties of soft magnetic FeCo alloys, *Mater. Sci. Eng., A* 329–331 (2002) 325–333, [https://doi.org/10.1016/S0921-5093\(01\)01594-5](https://doi.org/10.1016/S0921-5093(01)01594-5).
- [6] K. Kawahara, M. Uehara, A possibility for developing high strength soft magnetic materials in FeCo-X alloys, *J. Mater. Sci.* 19 (1984) 2575–2581, <https://doi.org/10.1007/BF00550812>.
- [7] M. Muller, H. Grah, N. Mattern, B. Schnell, (FeCoNi)-ZrBCu base alloys, the influence of transition metal composition and heat treatment on structure and magnetic properties, *J. Magn. Mater.* 215–216 (2000) 437–439, [https://doi.org/10.1016/S0304-8853\(00\)00182-7](https://doi.org/10.1016/S0304-8853(00)00182-7).
- [8] D.B. Miracle, O.N. Senkov, A critical review of high entropy alloys and related concepts, *Acta Mater.* 122 (2017) 448–451, <https://doi.org/10.1016/j.actamat.2016.08.081>.
- [9] Y. Zhang, T.T. Zuo, Z. Tang, M.C. Gao, K.A. Dahmen, P.K. Liaw, Z.P. Lu, Microstructures and properties of high entropy alloys, *Prog. Mater. Sci.* 61 (2014) 1–93, <https://doi.org/10.1016/j.pmatsci.2013.10.001>.
- [10] N.A. Morley, B. Lim, J. Xi, A. Quintana-Nedelcos, Z. Leong, Magnetic properties of the complex concentrated alloy system CoFeNi<sub>0.5</sub>Cr<sub>0.5</sub>Al<sub>x</sub>, *Sci. Rep.* 10 (2020), 14506, <https://doi.org/10.1038/s41598-020-71463-3>.

- [11] J. Harris, Z. Leong, P. Gong, J. Cornide, C. Pughe, T. Hansen, A. Quintana-Nedelcos, R. Rowan-Robinson, U. Dahlborg, M. Calvo-Dahlborg, R. Goodall, M. Rainforth, N. Morley, Investigation into the magnetic properties of  $\text{CoFeNiCr}_y\text{Cu}_x$  alloys, *J. Phys. D Appl. Phys.* 54 (2021), 395003, <https://doi.org/10.1088/1361-6463/ac1139>.
- [12] X. Jin, Y. Zhou, L. Zhang, X. Du, B. Li, A novel  $\text{Fe}_{20}\text{Co}_{20}\text{Ni}_{41}\text{Al}_{19}$  eutectic high entropy alloy with excellent tensile properties, *Mater. Lett.* 216 (2018) 144–146, <https://doi.org/10.1016/j.matlet.2018.01.017>.
- [13] F. Körmann, D. Ma, D.D. Belyea, M.S. Lucas, C.W. Miller, B. Grabowski, M.H. F. Sluiter, “Treasure maps” for magnetic high-entropy-alloys from theory and experiment, *Appl. Phys. Lett.* 107 (2015), 142404, <https://doi.org/10.1063/1.4932571>.
- [14] P. Li, A. Wang, C.T. Liu, Composition dependence of structure, physical and mechanical properties of  $\text{FeCoNi}(\text{MnAl})_x$  high entropy alloys, *Intermetallics* 87 (2017) 21–26, <https://doi.org/10.1016/j.intermet.2017.04.007>.
- [15] V.S. Hariharan, A. Karati, T. Parida, R. John, D.A. Babu, B.S. Murty, Effect of Al addition and homogenization treatment on the magnetic properties of  $\text{CoFeMnNi}$  high entropy alloy, *J. Mater. Sci.* 55 (2020) 17204–17217, <https://doi.org/10.1007/s10853-020-05171-8>.
- [16] T. Zuo, M.C. Gao, L. Ouyang, X. Yang, Y. Cheng, R. Feng, S. Chen, P.K. Liaw, J. A. Hawk, Y. Zhang, Tailoring magnetic behaviour of  $\text{CoFeMnNiX}$  ( $X = \text{Al, Cr, Ga}$  and  $\text{Sn}$ ) high entropy alloys by metal doping, *Acta Mater.* 130 (2017) 10–18, <https://doi.org/10.1016/j.actamat.2017.03.013>.
- [17] Y. Ma, B. Jiang, C. Li, Q. Wang, C. Dong, P. Liaw, F. Xu, L. Sun, The BCC/B2 morphologies in  $\text{Al}_x\text{NiCoFeCr}$  high-entropy alloys, *Metals* 7 57 (2017), <https://doi.org/10.3390/met7020057>.
- [18] S. Uporov, V. Bykov, S. Pryanichnikov, A. Shubin, N. Uporova, Effect of synthesis route on structure and properties of  $\text{AlCoCrFeNi}$  high-entropy alloy, *Intermetallics* 83 (2017) 1–8, <https://doi.org/10.1016/j.intermet.2016.12.003>.
- [19] A. Quintana-Nedelcos, M. Anis, R. Osman, J. Yang, Z. Leong, Y. Azakli, N. A. Morley, On the structural, microstructural and magnetic properties evolution of  $\text{Ni}_{0.5}\text{FeCoAlCr}_x$  alloys, *Mater. Lett.* 311 (2022), 131542, <https://doi.org/10.1016/j.matlet.2021.131542>.
- [20] N.W. Ashcroft, N.D. Mermin, *Solid State Physics*, Saunders College, Philadelphia, 1976.
- [21] Wei Li, Ping Liu, Peter K. Liaw, Microstructures and properties of high-entropy alloy films and coatings: a review, *Mater. Res. Lett.* 6 (4) (2018) 199–229, <https://doi.org/10.1080/21663831.2018.1434248>.
- [22] A. Takeuchi, A. Inoue, Mixing enthalpy of liquid phase calculated by miedema’s scheme and approximated with sub-regular solution model for assessing forming ability of amorphous and glassy alloys, *Intermetallics* 18 (9) (2010) 1779–1789, <https://doi.org/10.1016/j.intermet.2010.06.003>.
- [23] Z. Leong, H. Yuhe, R. Goodall, I. Todd, Electronegativity and enthalpy of mixing biplots for High Entropy Alloy solid solution prediction, *Mater. Chem. Phys.* 210 (2018) 259–268, <https://doi.org/10.1016/j.matchemphys.2017.09.001>.
- [24] L. Kraus, V. Soyka, P. Duhaj, Mat’ko, Magnetic properties of nanocrystalline  $\text{CoFeNbB}$  alloys, *J. Phys. IV France* (1998), [https://doi.org/10.1051/jp4:1998222\\_08](https://doi.org/10.1051/jp4:1998222_08), Pr2-95-Pr2-98.
- [25] <https://metglas.com/>.